The 11th Canadian Conference on Earthquake Engineering
Canadian Association for Earthquake Engineering

TOWARDS A RAPID SEISMIC RISK ASSESSMENT TOOL FOR CANADA

Alex SMIRNOFF
Geoscience Programmer, Geological Survey of Canada, Natural Resources Canada, Canada
alex.smirnoff@RNCan-NRCan.gc.ca

Ahmad ABO EL EZZ
Postdoctoral Fellow, Ecole de Technologie Supérieure Montréal, Canada
ahmad.abo-el-ezz.1@ens.etsmtl.ca

Marie-José NOLLET
Professor, Ecole de Technologie Supérieure Montréal, Canada
marie-jose.nollet@etsmtl.ca

Miroslav NASTEV
Scientific Researcher, Geological Survey of Canada, Natural Resources Canada, Canada
miroslav.nastev@RNCan-NRCan.gc.ca

ABSTRACT: Seismic risk assessment is the key component of the disaster resilience planning process in earthquake prone areas. In the last decades, the US FEMA's loss assessment methodology HAZUS-MH has become a de facto standard due to its well developed and widely accepted analytical approach for damage and loss calculations. In practice, preparing the necessary input layers and running the iterative approach for calculating the performance point of structures can be time consuming, and require advanced knowledge of GIS. As an alternative, a prototype of a rapid risk assessment tool, based on the same structural parameters but with a different computation algorithm, was developed. The tool meets the needs of the target groups of non-expert emergency management and public safety decision makers through easily understandable input and output information and flexible interactive environment, while maintaining the scientific rigour. It uses a database with pre-calculated vulnerability curves defined as functions of the intensity of the seismic shaking to evaluate the structural and non-structural damage state probabilities, casualties and economic losses. Results from numerous validation tests were compared with those from HAZUS-MH to confirm the accuracy of the method.

1. Introduction

In Canada, severe natural hazards such as large earthquakes are typically irregular events and those which lead to catastrophic consequences are relatively rare. Still, rare disastrous events happen and if not adequately addressed, the loss of life and property can be enormous. The conventional knowledge of the hazard information alone such as type, intensity and frequency is not sufficient for informed decision-making. In earthquake prone areas, the seismic risk assessment process is thus central to planning mitigation, preparedness and emergency response measures and achieving the overall safety. Numerous computer models are available for seismic risk analyses, such as OpenQuake (GEM 2015), SELENA (NORSAR 2015) or HAZUS-MH (FEMA-NIBS 2012a). The later has become a de facto standard due to its well developed and widely accepted analytical approach for damage and loss calculations. However, this program is intended for use by a small number of technical and scientific experts. HAZUS-MH can be used in Canada provided that local hazard and inventory databases are available. In practice, it involves intensive data preparation and processing of the results and advanced knowledge of GIS. It is therefore

ill-suited for application by the broader non-expert public safety community. As such communicating seismic risk to local stakeholders, so that they can indeed understand their exposure and vulnerability, represents an outstanding challenge.

Knowledge of exposure and vulnerability is the first prerequisite to any mitigation initiative. Recently, École de Technologie supérieure has partnered with Natural Resources Canada (NRCan) with the objective to develop seismic risk assessment methods and tools for simplified dynamic response of exposed structures, and seismic vulnerability evaluation. These efforts led to the development of EVARISK, a seismic risk assessment tool for the assessment of structural and non-structural damage to buildings. Currently, a multi-institutional and multi-disciplinary team focuses on accelerating of the standardized method for rapid seismic risk assessment, including near real-time generation of ground motions considering local site effects.

This paper presents the theoretical background behind the rapid seismic assessment and its implementation in a simple interface with out-of-the-box capacity, which can be run by a simple 'push of the button'. A comparison with damages estimates from the well-known HAZUS-MH (FEMA-NIBS 2012a) to ascertain the capability of EVARISK to assess seismic risk is also presented.

2. Theoretical background of the rapid seismic risk assessment tool

2.1. General framework of seismic risk evaluation

Seismic risk assessment at urban or regional scales involves seismic hazard, inventory of assets at risk and respective vulnerability. Vulnerability refers to the susceptibility to earthquake impacts defined by the potential physical damage and resulting economic and social losses. Central to the vulnerability modelling is the concept of a fragility function assumed as representative for a group of buildings with similar structural properties. Fragility functions combine the expected damage states in terms of the intensity of the seismic motion, referred to as intensity measure (IM).

Fig. 1 shows the general framework for the development of the rapid seismic risk assessment tool including the following major steps: (i) definition of earthquake scenario in terms of IM (e.g., spectral acceleration close to the natural vibration period of the buildings); (ii) inventory of existing buildings types; and (iii) vulnerability modelling applying the seismic hazard-compatible fragility functions.

The final output is the probability of the building components (structural system, acceleration-sensitive and drift-sensitive non-structural components) to be in each of the five damage states: none, slight, moderate, extensive, complete. Based on these probabilities, indoor casualties in four severity levels and economic losses sustained by building components and contents are also calculated using inventory information on occupancy class, replacement cost and number of occupants (Fig. 1).

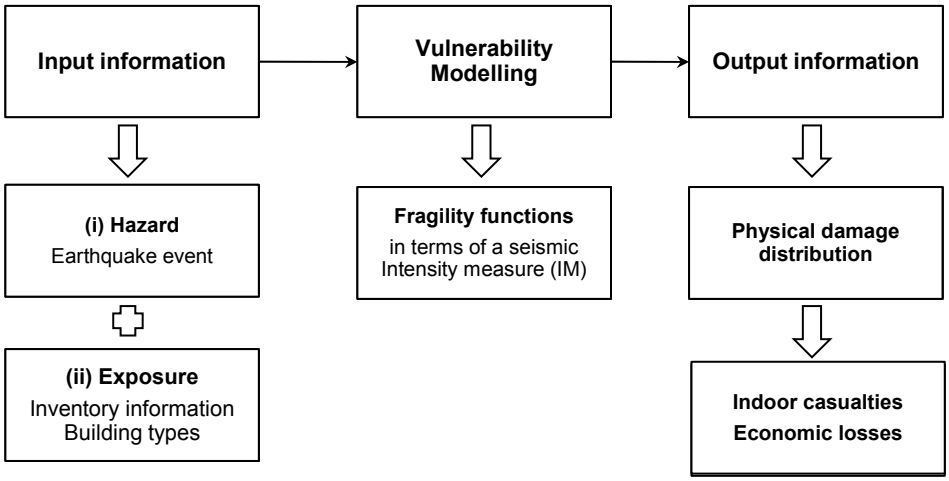

Fig. 1 – General framework for seismic risk assessment

EVARISK includes structural parameters and occupancy classes as defined in Hazus-MH (FEMA-NIBS 2012b). Although the applied general procedure is similar to the one implemented in HAZUS-MH, prediction of the seismic demand is performed using a different algorithm (Porter 2009a). The main characteristic of EVARISK still resides in its objective to meet the needs of the target groups of non-expert emergency management and public safety decision makers through easily understandable input and output information and flexible interactive environment while maintaining the scientific rigour.

2.2. Seismic displacement demand

The prediction of potential damage to buildings relies on the comparison of the structural response under seismic loading, the capacity curve, to the seismic demand of a given earthquake scenario, the demand spectrum (Fig. 2). Capacity curve describes the nonlinear structural behaviour under seismic loading obtained from pushover analysis. It is defined as a relationship between the lateral load and respective top displacement (Kircher et al, 1997; ASCE-41, 2013). As buildings are generally modelled with a simple equivalent single-degree-of-freedom (ESDOF) system, the capacity curve is also defined in the same domain as the demand spectrum, i.e., as spectral acceleration (lateral seismic force) vs. spectral displacement (structural deformation) relationship. Capacity curve typically consists of: a linear portion up to the yield point, representing the outset of eventual structural damage (Sa_y, Sd_y); an intermediate elliptical degrading-stiffness portion bounded by the ultimate point (Sa_u, Sd_u) at which the maximum lateral strength of the building is attained; and final part beyond the ultimate point where displacement occurs without increase of the seismic force (Fig. 2). The parameters of the capacity curves developed for generic building types (Sa_y, Sd_y, Sa_u and Sd_u) are extracted from the HAZUS-MH technical manual (FEMA-NIBS 2012b). From the structural point of view, there are 36 major building types depending on the construction material (wood, steel, concrete, masonry and manufactured housing), lateral force resisting system (bearing wall, shear wall, frame, etc.), and building height (low: 1-3 storeys, medium: 4-7 storeys, and high-rise: 8+ storeys). The apparent resistance to seismic loads for each building class is assigned with one of the four available design criteria (pre-code, low-code, moderate-code, and high-code), mainly functions of the year of construction and regional seismic hazard, resulting in a total of 128 building types.

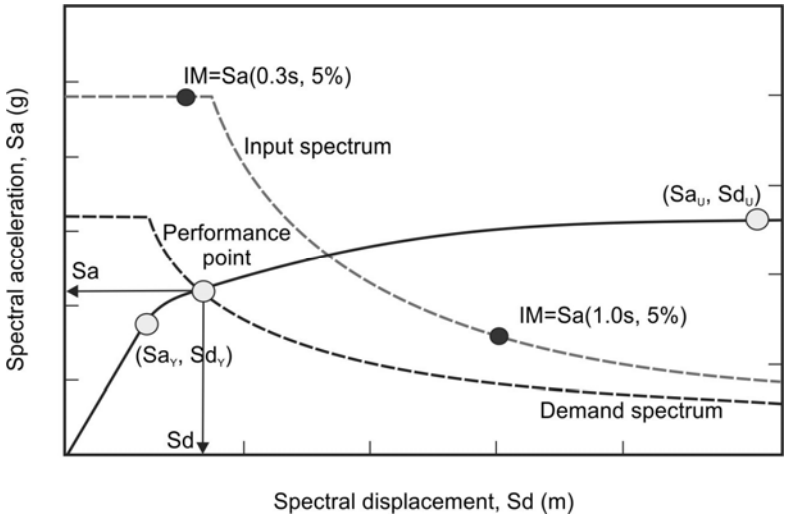

Fig. 2 – Capacity curve and demand spectrum for prediction of the seismic demand

The first part of the vulnerability modelling for a specific building type conducted in this study was inspired by the standard framework for performance-based engineering (Moehle and Deierlein 2004, Porter, 2009a; FEMA-NIBS 2012a). Two dominant spectral accelerations at 0.3 and 1.0 seconds (Sa(0.3s) and Sa(1.0s)) are used as IMs for buildings with a short and long period of vibration, respectively. They fully define a simplified 5%-damped input response spectrum for a given seismic scenario including local soil conditions (Fig. 2). The maximal structural response of the considered building type, referred to as the 'performance point', is determined by the intersection between its structural capacity curve and the

response spectrum adjusted for the inelastic structural damping associated with cyclic degradation (Kircher et al. 1997) using the capacity spectrum method (CSM) (Mahaney et al., 1993; ATC 40, 1996).

To simplify the damage assessment and avoid the iterative process involved in determination of the performance point, an alternate solution process is adopted that relies on a set of fragility curves expressed as explicit functions of the input intensity measure (Porter 2009a). These functions are determined for different earthquake scenario by applying a "backward algorithm". The first step consists in assuming a performance point (Sd, Sa, ξ_{eff}) on the idealized response spectrum with effective damping ratio, referred to as 'demand spectrum'. Considering the effects of damping, the demand spectrum is then related to the standard 5% damped response spectrum adjusted to the local soil conditions referred to as 'index spectrum'. The index spectrum is defined by the spectral acceleration at 0.3sec, Sa(0.3s, 5%), associated with stiffer low-rise buildings (short period range), and the spectral acceleration at 1.0sec, Sa(1.0s, 5%), associated with taller and more flexible buildings (long period range). These two spectral accelerations represent the standard structure-independent IMs. Their values are obtained from the index response spectrum using the spectral reduction factor relationship according ATC-40 (1996).

2.3. Displacement Fragility functions

In the second step (forward computation), the spectral displacement (Sd) of the performance point is compared with a set of displacement based fragility functions characteristic for the respective generic building type to obtain the probability of being in each of the four predefined damage states, e.g., none, slight, moderate, extensive and complete (Coburn and Spence, 2002; Kircher et al, 1997). The displacement fragility functions are given as lognormal distribution functions conditioned on a threshold structural response parameter, the inelastic spectral displacement demands (S_d), that represent the earthquake induced displacement of the ESDOF model of the building (Fig. 3). Then, the probabilistic damage states are correlated with the respective IM defined by the input spectrum, Sa(0.3s, 5%) or Sa(1.0s, 5%). This procedure allows for direct evaluation of the expected structural, non-structural and content damage given a ground motion scenario.

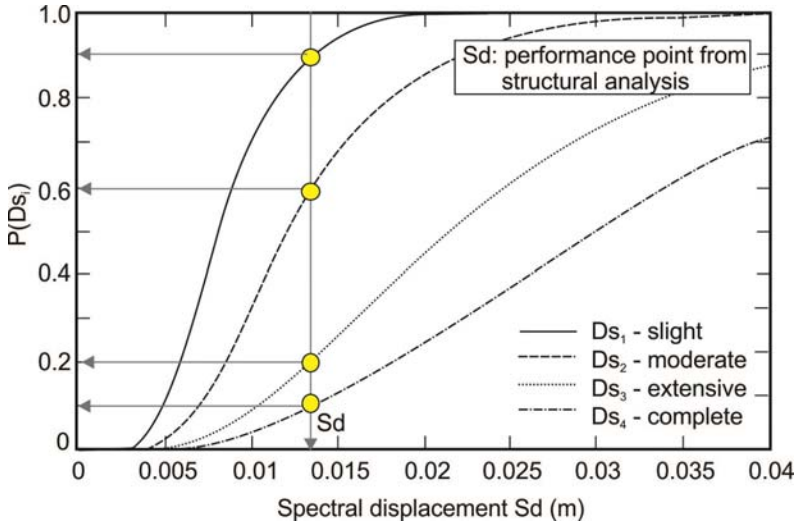

Fig. 3 – Displacement fragility functions for structural damage of low-rise pre-code unreinforced masonry building class.

To establish a database of performance points which correlate the input IMs to damage estimates, the procedure was repeated by gradually increasing shaking intensity. The process starts with low IM yielding displacement response close to zero, and finishes with highest possible IM for that location resulting to the ultimate point on the capacity curve. The respective probabilistic damage states are computed for each successive step and arranged in tabular format together with the associated intensity. An example of computation results is presented in Table 1. A simple calculation algorithm was written to accelerate the computation of the probability of exceedance of damage states conditioned to the IM.

Once developed, the database of damage states conditioned to input IMs can readily be used for assessing expected building damage and corresponding economic and social losses for any potential level of seismic shaking (magnitude-distance scenarios). This is the main characteristic of the proposed procedure and the whole process can be configured to automatically generate geospatial maps of seismic shaking and resulting damage immediately following a strong earthquake.

Table 1 – Example computation results for the performance point and the corresponding IM and structural component damage state probabilities.

Performance point		**IM from input spectrum**	**Probability of exceedance of damage states**			
Sd (mm)	Sa (g)	Sa(0.3s) (g)	Slight	Moderate	Extensive	Complete
0.25	0.008	0.013	0.000	0.000	0.000	0.000
0.40	0.013	0.020	0.001	0.000	0.000	0.000
0.63	0.021	0.032	0.003	0.000	0.000	0.000
0.80	0.026	0.040	0.006	0.001	0.000	0.000
1.01	0.033	0.050	0.011	0.001	0.000	0.000
1.60	0.053	0.079	0.034	0.004	0.000	0.000
2.01	0.066	0.100	0.055	0.008	0.000	0.000
2.54	0.083	0.125	0.085	0.014	0.001	0.000
3.19	0.105	0.158	0.126	0.024	0.001	0.000
4.02	0.132	0.199	0.180	0.040	0.003	0.000
5.06	0.166	0.250	0.246	0.062	0.005	0.000
6.38	0.209	0.315	0.323	0.094	0.009	0.001
8.03	0.246	0.400	0.408	0.136	0.017	0.001
10.11	0.279	0.498	0.498	0.190	0.028	0.003
16.02	0.343	0.750	0.674	0.330	0.069	0.010
20.17	0.377	0.826	0.752	0.413	0.102	0.017
31.97	0.447	1.189	0.872	0.587	0.201	0.045
40.25	0.483	1.602	0.914	0.670	0.266	0.070

Note: Intermediate values of performance points have been removed for concision

3. Algorithm and programing

The development of EVARISK followed three distinct steps: (i) implementation of the backward algorithm meant to associate damage state probabilities and indoor casualties to IMs, as presented in Section 2 and shown in Fig. 4 (*Step 1*); (ii) generation of a database tabulating the associated values for different earthquake scenarios (Fig. 4, *Step 2*); and (iii) development of an interface which refers to the database to provide rapid risk assessment for individual building types in different scenarios (Fig. 5). Each step is described in more details below.

To implement the algorithm, capacity- and fragility-curve parameters for 128 building types (36 structural types x 4 design codes) were extracted from the HAZUS-MH technical manual (FEMA-NIBS 2012b) and stored in a PostgreSQL database table. Then, a tool for calculating the IMs based on a selected Sd value and mapping them to damage state probabilities for four structural and non-structural damage states was designed and programed in Java. Based on structural damage, the tool also calculates the probabilities of indoor injuries in four categories (slight, moderate, severe and fatal).

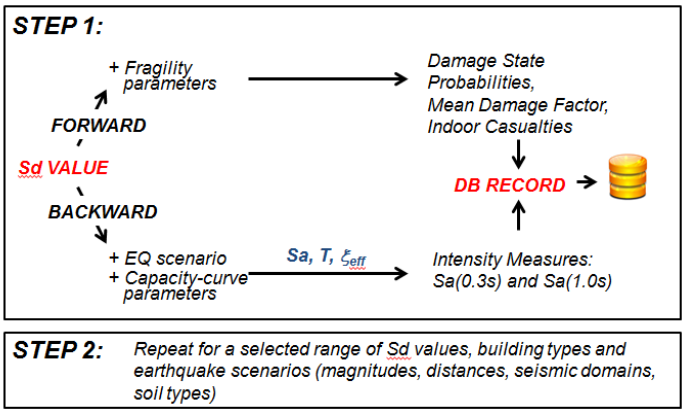

Fig. 4 – Development of EVARISK: Steps 1 and 2

The tool was then used to generate vulnerability functions from equally logarithmically spaced Sd values ranging from 10^{-2} to 10^{3} in, for each building type in 100 earthquake scenarios. The scenarios are represented by permutations of four magnitudes (M5, M6, M7, M8) five distances (10, 20, 30, 40 and 60km) and five NEHRP site classes (A, B, C, D, E). The generated vulnerability functions were then tabulated in a PostgreSQL database. Three separate tables were created based on different ground motion prediction equations (GMPE) and simple point source model (Boore et al. 1997, Atkinson and Boore 2006, Atkinson and Adams 2013).

The simple interface that runs as a Java applet or desktop application is shown in Fig. 5. The user selects a scenario including domain (Eastern North America – ENA or Western North America – WNA), GMPE, magnitude, epicentral distance, soil type, building type, occupancy class, replacement cost, and the number of occupants. First, Sa(0.3s) and Sa(1.0s) are calculated based on the selected scenario and GMPE. Then, a query is send to the database for the selected building type using the value of primary IM and the input scenario. The damage and human loss estimates are obtained through interpolation between two closest tabulated IM values. In addition to the data retrieved from the database, the tool calculates economic loss in all categories. The mean damage factor (Porter, 2009b) and coefficient of variation (Porter, 2010) are also calculated and reported. The results are tabulated, presented graphically and can be saved in a report file.

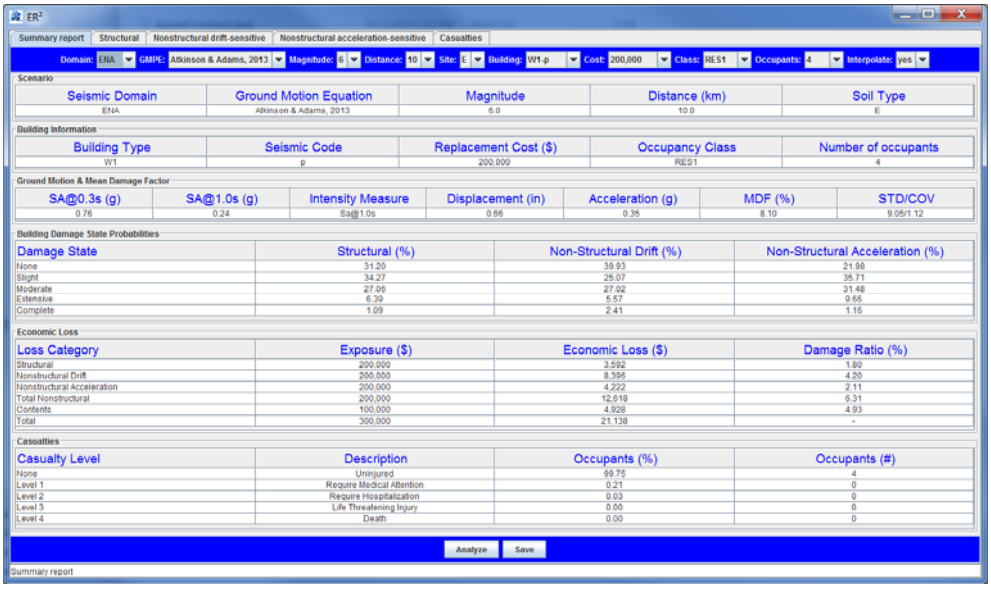

Fig. 5 – EVARISK toolbar for input parameters (top), and the standard 'Summary Report' form (bottom)

4. Validation

Damage estimates in EVARISK rely on an algorithm different from the one implemented in HAZUS-MH. However, as both tools use the same basic capacity and fragility parameters, it is expected that structural and non-structural damage state probabilities and other derived results, such as casualties and economic loss, should remain generally coherent.

4.1. Comparison of damage state probabilities and casualties

The validation was conducted by comparing the probabilities obtained from EVARISK with the results from HAZUS-MH, while applying identical input values for Sa(0.3s), Sa(1.0s) and PGA. A total of 3,840 tests were performed in each damage/loss category resulting from the analysis of 128 building types on 5 NEHRP site classes (A, B, C, D, E) for 3 magnitudes (M6, M7, M8) and 2 distances (10km, 20 km). These tests were repeated for structural damage, non-structural acceleration-sensitive damage, non-structural drift-sensitive damage and indoor casualties to a grand total of 15,360 tests.

Table 2 – Deviations between EVARISK and HAZUS-MH damage probabilities based on 3,840 tests per damage/loss category.

	Structural damages			Non-structural drift-sensitive damages			Non-structural acceleration-sensitive damages		
	M6	**M7**	**M8**	**M6**	**M7**	**M8**	**M6**	**M7**	**M8**
Overall average deviation	0.22%	0.59%	1.03%	0.22%	0.93%	2.83%	3.32%	5.62%	9.63%
Number of tests with average deviations >5%	0	0	0	0	0	29	9	77	104
Overall maximum deviation	6.16%	5.20%	11.81%	4.62%	20.93%	39.61%	31.84%	35.16%	68.49%
Number of tests with maximum deviation >10%	0	0	4	0	21	54	124	127	128

Deviation from HAZUS-MH results was computed for the above four damage/loss categories as a measure of accuracy. The "*No damage*" state was not considered in the comparison, and the *"Complete damage"* and *"Complete damage with collapse"* states calculated by EVARISK were merged into a single state referred to as "*Complete damage"*. Table 2 presents the overall average and maximum deviations for structural and non-structural damages. In general, the results show a better correlation for lower magnitudes. For structural damage, the overall average deviation is slightly over 1% with only 4 tests deviating marginally over 10%. For non-structural damage, results show greater deviations and depend on whether the damage is derived for drift- or acceleration-sensitive components. For non-structural drift-sensitive damage, the overall average deviation is below 3% with 54 tests exceeding 10%, which is still deemed reasonable. However, deviations for non-structural acceleration-sensitive components are often greater than 10% even at lower magnitudes. The latter results are investigated in more detail in Section 4.2. Similar comparisons for indoor injuries demonstrate very favorable results. The overall maximum deviation in one of M8 scenarios was as low as 0.87%, with the average deviation over the entire series of tests being as low as 0.03%.

In addition to damage state probabilities, mean damage factors (MDF), as described in Porter (2009b), were computed. A total of 4,200 tests were performed for: 5 building types *(W1-p, W1-m, URML-p, S1L-p, S2L-p)*, 28 HAZUS occupancy classes, 5 NEHRP site classes (A, B, C, D, E), 3 magnitudes (M6, M7, M8) and 2 distances (10km, 20 km). As HAZUS-MH does not explicitly report the MDF, these results could not be compared. However, trends in the coefficient of variation (COV) and standard deviation (STD) of MDF were analysed and compared with the results previously reported by Porter (2010). Fig. 6 shows the distribution of COV and STD versus the MDF, with a R^2 of 0.9562 and 0.9787 for the respective trend-lines. These results are consistent with those reported by Porter (2010) indicating similar

trends and R^2 values, 0.93 and 0.97 respectively. As seen from Fig. 6, the coefficient of variation decreases with an increase in MDF while the standard deviation slightly increases with MDF which is characteristic of analytical vulnerability methodologies (Porter 2010, Porter et al. 2006).

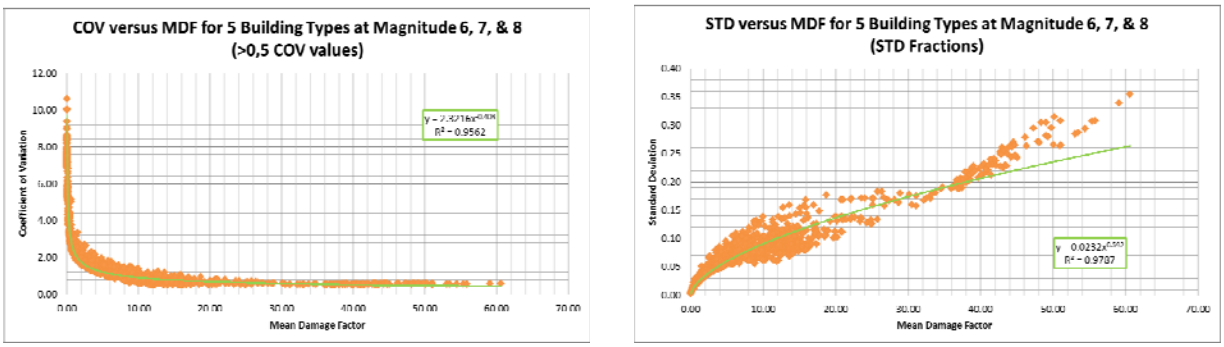

Fig. 6 – Analysis of uncertainty (COV and STD) in the MDF calculated by EVARISK

4.2. Comparison of HAZUS-MH and EVARISK acceleration-sensitive components

To understand the relatively high deviations for non-structural acceleration-sensitive damage, the performance point (PP) parameters Sa@PP and Sd@PP were compared for the input capacity curves of five selected building types: URML-PC, URMM-PC, S5L-PC, C1L-PC, and W1-PC (Fig. 7). In the capacity spectrum method, the computed performance point lies on the capacity curve and the Sa@PP cannot exceed the ultimate acceleration of the capacity curve.

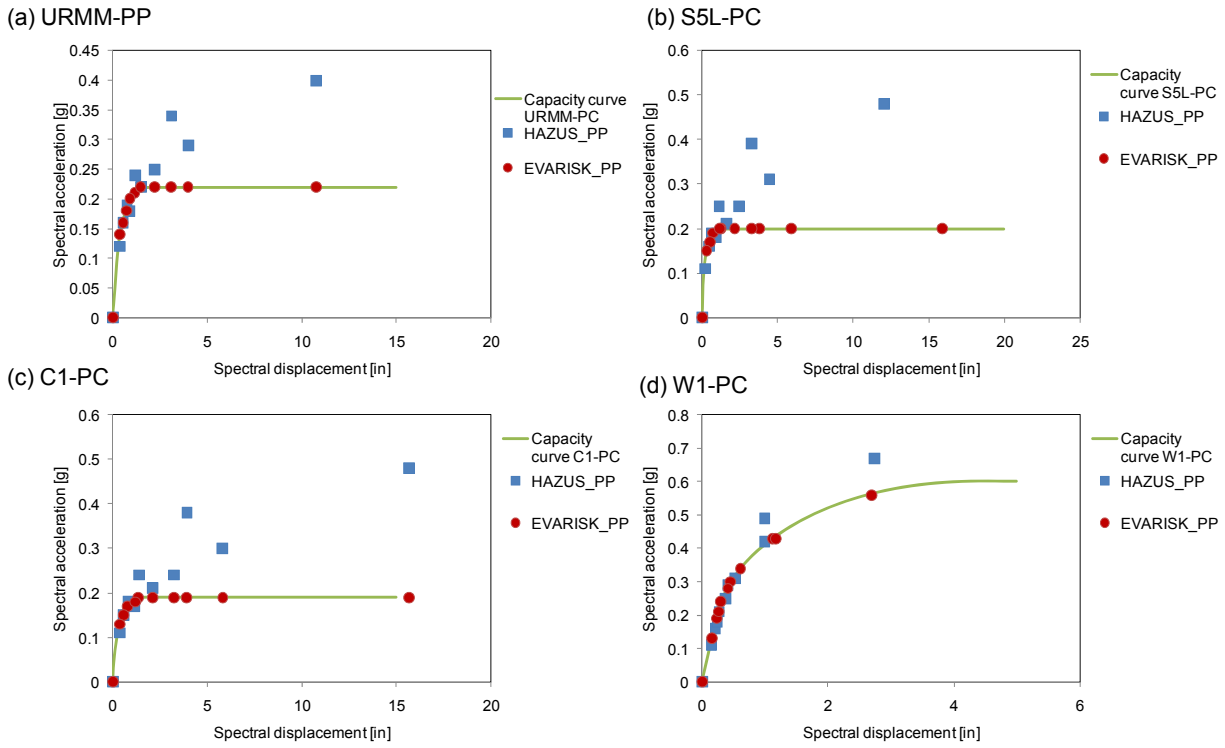

Fig. 7 – Capacity curves for acceleration sensitive components and the corresponding performance points for the selected scenarios.

As shown in the Fig. 7, the predicted PP parameters using EVARISK are all located on the input capacity curve. However, in HAZUS-MH results, the PPs depart slightly from the capacity curve for low seismic demands with gradually increasing deviations for higher seismic demands. This overestimation of the

Sa@PP results in overestimation of the predicted non-structural acceleration sensitive components. As discussed above, in EVARISK, the computation process starts with assumed PP parameters which coincide with a point on the capacity curve, and then backward and forward calculations are conducted to correlate the IMs to the damage states. On the other hand, HAZUS-MH computation starts with the input IMs to obtain the PP parameters using an iterative procedure, and then a forward computation is applied to obtain the damage states. The above differences in general approach could potentially result in the observed deviations in damage estimates for acceleration sensitive components.

5. Conclusion

The theoretical background behind the recently developed seismic risk assessment tool EVARISK was presented. Its main characteristic is easily understandable input and output information and flexible interactive environment, which contribute to meet the needs of the non-expert emergency management and public safety decision makers to understand their exposure and perform own risk assessments. The general framework includes the definition of earthquake scenario in terms structure independent IM determined as spectral acceleration close to the natural vibration period of the buildings, and the vulnerability modelling. The computation process is similar to the one implemented in HAZUS-MH, but the prediction of the seismic demand applies a different algorithm programmed in Java. It first calculates the IM values based on selected performance points, and the IMs are then correlated to damage state probabilities. Capacity- and fragility-curve parameters for 128 building types are stored in a PostgreSQL database table. A simple interface that runs as a Java applet or desktop application allows the selection of an earthquake scenario for Eastern or Western North America, and the results are tabulated, represented graphically and can be saved in a report file. The validation process consisted in comparison of obtained damage probabilities with those from HAZUS-MH, in a total of 15,360 tests. The results are almost identical for indoor casualties with a maximum deviation of 0.87%. The structural damage probabilities comparisons show also excellent agreement with an average deviation slightly over 1%. The non-structural damage probabilities for drift- and acceleration-sensitive components, however, show relatively high deviations. In general, the results show better correlations for lower intensity of ground shaking. To understand the relatively high deviations between HAZUS-MH and EVARISK results are obtained for non-structural acceleration-sensitive damage, the performance point parameters (PP) were compared for the input capacity curves of selected building types.

6. Acknowledgements

This work was partially supported by the NRCan's Public Safety Geoscience Program and by the Canadian Safety and Security Program (CSSP) which is led by Defense Research and Development Canada's Centre for Security Science, in partnership with Public Safety Canada. The CSSP is a federally-funded program to strengthen Canada's ability to anticipate, prevent/mitigate, prepare for, respond to, and recover from natural disasters, serious accidents, crime and terrorism through the convergence of science and technology with policy, operations and intelligence.

7. References

ASCE. ASCE 41-13 Seismic Evaluation and Retrofit of Existing Buildings. American Society for Civil Engineering, Virginia, USA, 2013.

ATC. Seismic evaluation and retrofit of concrete buildings: ATC-40. Applied Technology Council, Redwood City, California, USA, 1996.

ATKINSON, G.M. and BOORE, D.M, "Earthquake ground-motion prediction equations for eastern North America", *Bulletin of the Seismological Society of America,* Vol. 96, No. 6, 2006, pp. 2181-2205.

ATKINSON, G.M. and ADAMS, J. "Ground motion prediction equations for application to the 2015 Canadian national seismic hazard maps", *Canadian Journal of Civil Engineering*, Vol. 40, 2013, pp. 988-998.

BOORE, D.M., JOYNER, W.B. and FUMAL, T.E. "Equations for estimating horizontal response spectra and peak acceleration from Western North American earthquakes: A summary of recent work", Seismological research letters, Vol. 68, No. 1, 1997, pp. 128-153. And Erratum.

COBURN, A. and SPENCE, R. Earthquake Protection, 2nd edition, New York: John Wiley & Sons, Inc., 2002.

FEMA (Federal Emergency Management Agency). (2012). "Hazus-MH 2.1 – Earthquake Model User Manual." Washington, D.C.,

FEMA-NIBSa. HAZUS-MH 2.1: Multi-hazard Loss Estimation Methodology Earthquake Model. User Manual, Federal Emergency Management Agency, National Institute of Building Science, Washington, D.C, USA. 2012, 863 p.

FEMA-NIBSb. HAZUS-MH 2.1: Multi-hazard Loss Estimation Methodology Earthquake Model. Technical manual, Federal Emergency Management Agency, National Institute of Building Science, Washington, D.C, USA. 2012, 718 p.

GEM (Global Earthquake Model). "Openquake Platform". Pavia, Italy, <https://github.com/gem/oq-platform>, February 2015.

KIRCHER, C. A., NASSAR, A. A., KUSTU, O., and HOLMES, W. T. "Development of building damage functions for earthquake loss estimation", *Earthquake spectra*, Vol. 13, No. 4, 1997, pp. 663-682.

MAHANEY, A., PARET, T.F., KEHOE, B.E. and FREEMAN, S.A. "The Capacity Spectrum Method for Evaluating Structural Response during the Loma Prieta Earthquake", *Proceedings of the 1993 United States National Earthquake Conference*, Memphis, Tennessee, USA, Vol. 2, 1993, pp. 501-510.

MOEHLE, J., and DEIERLEIN, G. G. "A framework methodology for performance-based earthquake engineering", *Proceedings, 13th World Conference on Earthquake Engineering*, Vancouver, Canada, 2004, 13 p.

NORSAR. "Risk Analysis Software – The SELENA-RISe open Risk Package". Kjeller, Norway, 〈http://www.norsar.no/seismology/engineering/SELENA-RISe/〉, April 2015.

PORTER, K. A., SCAWTHORN, C.R. and BECK, J.L. "Cost-effectiveness of stronger woodframe buildings", *Earthquake Spectra*, Vol. 22, No. 1, 2006, pp. 239-266.

PORTER, K. A. "Cracking an open safe: HAZUS vulnerability functions in terms of structure-independent spectral acceleration", *Earthquake Spectra*, Vol. 25, No. 2, 2009a, pp. 361–378.

PORTER, K. A. "Cracking an open safe: More HAZUS vulnerability functions in terms of structure-independent intensity", *Earthquake Spectra*, Vol. 25, No. 3, 2009b, pp. 607–618.

PORTER, K. A. "Cracking an open safe: Uncertainty in HAZUS-based seismic vulnerability functions", *Earthquake Spectra*, Vol. 26, No. 3, 2010, pp. 893-900.